10
Space Solar Cells and Arrays

Sheila Bailey[1] and Ryne Raffaelle[2]

[1]*NASA Glenn Research Center, Cleveland, OH, USA,* [2]*Department of Physics, Rochester Institute of Technology, Rochester, NY, USA*

10.1 THE HISTORY OF SPACE SOLAR CELLS

10.1.1 Vanguard I to Deep Space I

In the mid 1950s, the development of single-crystal photovoltaic (PV) solar cells based on Si, as well as GaAs, had reached solar conversion efficiencies as high as 6% [1, 2]. By 1958, small-area silicon solar cells had reached an efficiency of 14% under terrestrial sunlight. These accomplishments opened the door to the possibility of utilizing solar power on board a spacecraft. On March 17, 1958 the world's first solar-powered satellite was launched, Vanguard I [3]. It carried two separate radio transmitters to transmit scientific and engineering data concerning, among other things, performance and lifetime of the 48 p/n silicon solar cells on its exterior. The battery powered transmitter operated for only 20 days, but the solar cell powered transmitter operated until 1964, at which time it is believed that the transmitter circuitry failed. Setting a record for satellite longevity, Vanguard I proved the merit of space solar cell power. The solar cells used on Vanguard I were fabricated by Hoffman Electronics for the US Army Signal Research and Development Laboratory at Fort Monmouth. In 1961, many of the staff from the silicon cell program at Fort Monmouth transferred to the National Aeronautics and Space Administration (NASA), Lewis Research Center (now Glenn Research Center) in Cleveland, Ohio. From that time to the present, the Photovoltaic Branch at Glenn has served as the research and development base for NASA's solar power needs. Impressed by the light weight and the reliability of photovoltaics, almost all communication satellites, military satellites, and scientific space probes have been solar-powered. It should be noted that the history presented here focuses on the United States space program. NASA was created in 1958; the Institute of Space and Astronautical Sciences (ISAS) and the National Space Development Agency (NASDA) in Japan were created in 1965 and 1969, respectively;

Handbook of Photovoltaic Science and Engineering. Edited by A. Luque and S. Hegedus
 ISBN: 0-471-49196-9

the European Space Agency (ESA) was created in 1975 by the merger of the European Organization for the Development and Construction of Space Vehicle Launchers (ELDO) and the European Space Research Organization (ESRO), which had begun in the early sixties. There are notable achievements in photovoltaics from these multiple agencies.

As the first PV devices were being created, there were corresponding theoretical predictions emerging that cited ~20% as the potential efficiency of Si and 26% for an optimum band gap material (~1.5 eV) under terrestrial illumination [4]. In addition, it was not long before the concept of a tandem cell was proposed to enhance the overall efficiency. An optimized three-cell stack was soon to follow with a theoretical optimum efficiency of 37% [5]. Early solar cell research was focused on understanding and mitigating the factors that limited cell efficiency (e.g. minority carrier lifetime, surface recombination velocity, series resistance, reflection of incident light, and nonideal diode behavior).

The first satellites needed only a few watts to several hundred watts. They required power sources to be reliable and ideally to have a high specific power (W/kg), since early launch costs were ~$10 000/kg or more. The cost of the power system for these satellites was not of paramount importance since it was a small fraction of the satellite and the launch cost. The size of the array, and therefore the power, was limited for many early satellites owing to the body-mounted array design. Thus, there were multiple reasons to focus on higher-efficiency solar cells. Explorer I launched in 1958 discovered the van Allen radiation belts, adding a new concern for space solar cells (i.e. electron and proton irradiation damage). The launch of Telstar in 1962 also ushered in a new era for space photovoltaics (i.e. terrestrial communications) [6]. Telstar's beginning of life (BOL) power was 14 W but high radiation caused by the "Starfish" high-altitude nuclear weapon test reduced the power output [7]. This test caused a number of spacecraft to cease transmission. The lessons learnt from Explorer I and Telstar prompted a surge of activity in radiation protection of space solar cells and prompted the use of *n*-on-*p* silicon semiconductor type (rather than *p*-on-*n*) for superior radiation resistance. Radiation damage studies at the Naval Research Laboratories in the 1960s provided much in the way of guidance to spacecraft designers in accounting for cell degradation [8].

As communication satellites evolved throughout the 1960s, so did their power requirements and thus the size and mass of the solar arrays. There were some early attempts to address the issue of mass by developing thin-film cells such as CdS on Cu_2S heterojunction devices [9]. Unfortunately, their use was prohibited by severe degradation over time. CdTe cells were developed reaching efficiencies of ~7% [10]. However, the higher efficiency and stability of the silicon solar cells assured their preeminence in satellite power for the next three decades. Research on thin-film cells for space applications, because of their higher specific power and projected lower costs, is still an area of intense research today.

In 1973, the largest solar array ever deployed up to that time was placed in low-Earth orbit (LEO) of Skylab 1 [11]. Skylab was powered by the Orbital Workshop array and the Apollo Telescope Mount array. The orbital Workshop array had 2 deployable wings, each with 73 920 (2 cm × 4 cm) *n*-on-*p* Si cells that provided over 6 kW of power. Unfortunately, one of these wings was lost during launch. The Apollo Telescope Mount array had 4 wings with 123 120 (2 cm × 4 cm) cells and 41 040 (2 cm × 6 cm)

cells providing over 10 kW of power. The 1970s also saw the first use of shallow junction silicon cells for increased blue response and current output, the use of the back surface field, the low–high junction theory for increased silicon cell voltage output, and the development of wraparound contacts for high efficiency silicon (HES) cells to enable automated array assembly and to reduce costs.

In the 1980s, the gap between theoretical efficiencies and experimental efficiencies for silicon, gallium arsenide, and indium phosphide became almost nonexistent (see Figure 10.1) [12]. New thin-film cells of amorphous silicon and $CuInGaSe_2$ brought the possibility of higher thin-film efficiencies and flexible, lightweight substrates that excited the space community. However, silicon still provided the majority of the power for space and eventually the solar arrays for the International Space Station (ISS) (see Figure 10.2).

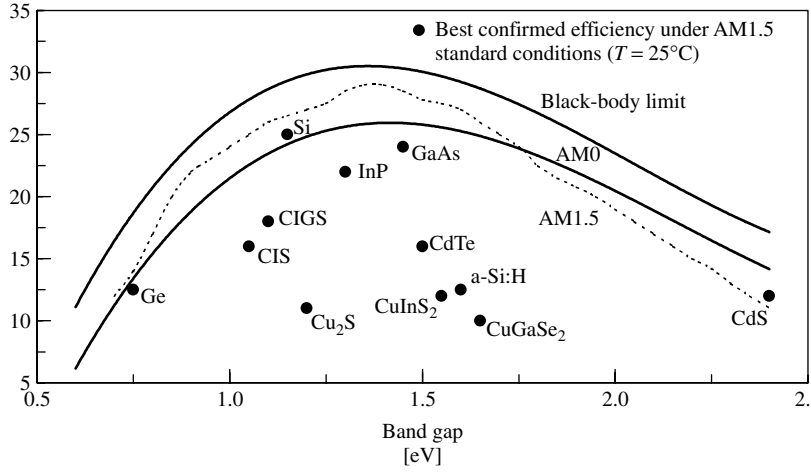

Figure 10.1 Comparison of measured cell efficiencies to the theoretical limits as a function of band gap [12]

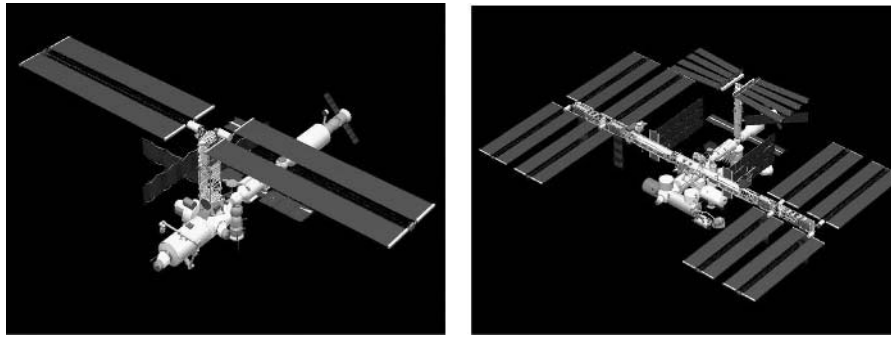

(a) (b)

Figure 10.2 (a) Current status of International Space Station (ISS) and (b) planned configuration of ISS by 2004. (Pictures courtesy of NASA)

Table 10.1 Summary of existing space solar cell performance [15] obtained at AM0

Parameter	Silicon	High-efficiency silicon	Single-junction GaAs	Dual-junction III-V	Triple-junction III-V
Status	Obsolete	SOA	Obsolete	Nearly obsolete	SOA
Efficiency (%)	12.7–14.8	16.6	19	22	26.8
Operating voltage (V)	0.5	0.53	0.90	2.06	2.26
Cell weight (kg/m^2)	0.13–0.50	0.13–0.50	0.80–1.0	0.80–1.0	0.80–1.0
Normalized efficiency temperature coefficient at 28°C	−0.55%/C	−0.35%/C	−0.21%/C	−0.25%/C	−0.19%/C
Cell thickness (μm)	50–200	76	140–175	140–175	140–175
Radiation tolerance	0.66–0.77	0.79	0.75	0.80	0.84
Absorptance (ratio of absorped radiant flux to the incident AM0 flux)	0.75	0.85	0.89	0.91	0.92

The ISS will have the largest PV power system ever present in space. It will be powered by 262 400 (8 cm × 8 cm) silicon solar cells with an average efficiency of 14.2% on 8 US solar arrays (each ~34 m × 12 m) [13]. This will generate about 110 kW of average power, which after battery charging, life support, and distribution, will supply 46 kW of continuous power for research experiments. The Russians also supply an additional 20 kW of solar power to ISS.

Space solar cell research in the 1990s focused on the III-V and multijunction (MJ) solar cells that had higher efficiencies and were more tolerant of the radiation environment. Satellites continued to grow in both size and power requirements and structures were designed to deploy large solar arrays. The mass and fuel penalty for attitude control of these large arrays continued to drive the space photovoltaics community to develop more efficient cells. Costs for satellite power systems remained at about a $1000/W.

The Deep Space 1 spacecraft, launched in October 1998, was the first spacecraft to rely upon SCARLET concentrator arrays to provide power for its ion propulsion engines [14]. Concentrator arrays use either refractive or reflective optics to direct concentrated sunlight onto a smaller active area of solar cells. Deep Space 1 had two such arrays and each was capable of producing 2.5 kW at 100 V (DC). The SCARLET arrays were developed by AEC-ABLE Engineering, Inc., under a program sponsored by the Ballistic Missile Defence Organization (BMDO). These arrays performed flawlessly under this inaugural demonstration.

The state-of-the-art (SOA) space solar cells available today are triple-junction III-V semiconductor cells. However, high-efficiency Si cells are still utilized in a number of space applications. Table 10.1 summarizes the SOA in space solar cells [15].

10.2 THE CHALLENGE FOR SPACE SOLAR CELLS

A team from NASA, Department of Energy (DOE), and the Airforce Research Laboratory (AFRL) engineers recently reviewed the power technology needs of mid- and

long-term proposed space science missions and assessed the adequacy of SOA solar cell and array technologies [16]. At present, while low-cost thin-film cells are just beginning to present a viable space power option [~10% air mass zero (AM0) efficiency for small-area cells], the best space solar cells are triple-junction III-V cells with an AM0 efficiency around 27%, and conventional arrays have reached a specific power of around 70 W/kg. These arrays meet the needs of many near-Earth missions but fail to meet some critical NASA Office of Space Science (OSS) mission needs in three ways. These are (1) missions that utilize solar electric propulsion (SEP) and require much higher specific power (150–200 W/kg), (2) missions that involve harsh environments [low solar intensity/low temperature, high solar intensities (HIHT), high-radiation exposure, and Mars environments], and (3) Sun–Earth connection missions that require electrostatically clean arrays that do not allow the array voltage to contact and thereby distort the plasma environment of the array. The entire surface of an electrostatically clean array is maintained at approximately the same potential as the spacecraft structure.

Work is in progress at several U.S. National Labs, universities, and solar cell companies to develop four-junction III-V cells with 30 to 35% efficiency and/or low-cost thin-film cells with large-scale efficiencies greater than 12%. This work is supported mainly by NASA, AFRL, and DOE [National Renewable Energy Lab (NREL)]. Unfortunately, no significant programs are presently under way to develop solar cells that can function efficiently in harsh environments. The majority of the ongoing work on advanced arrays is focused on developing flexible thin-film arrays. A limited amount of work is in progress on the development of concentrator arrays and electrostatically clean arrays. Table 10.2 compares space solar power (SSP) drivers and current SOA technology.

10.2.1 The Space Environment

All solar cells that are developed for use in space must take into consideration the unique aspects of the space environment. The spectral illumination that is available in space is not filtered by our atmosphere and thus is different from what is experienced on Earth. Space solar cells are designed and tested under an Air Mass Zero (AM0) spectrum (see Figure 16.1). A more complete discussion of air mass (AM) can be found in Chapters 16 and 20.

In the terrestrial PV world, cost is still the driver in PV development, and this has generated interest in several thin-film material systems (i.e. amorphous silicon, $CuInGaSe_2$, CdTe). The smaller material costs and higher production potential for thin-film arrays may well drive PV modules below current costs. The current National Photovoltaics Goal is the development of a 20% thin-film cell. The problem is more complicated for space applications since these cells must also be developed on a lightweight flexible substrate that can withstand the rigors of the space environment. This suggests that a minimum of 15% AM0 efficiency will be needed to be competitive with current satellite power systems. The current benchmark for the space PV world are commercially available multijunction III-V cells of GaInP/GaAs/Ge described further in Chapter 9. Table 10.3 lists the current status of cell efficiencies measured under standard conditions (AM1.5 global) as well as extraterrestrial (AM0) spectra.

The major types of radiation damage in solar cells that are of interest to designers are ionization and atomic displacement due to high-energy electrons and protons

Table 10.2 Comparison of technology requirements with state-of-the-art space solar cells [16]

Technology	Driving missions	Mission application	State of the art
High-power arrays for solar electric propulsion (SEP)	Comet nucleus sample return, outer planet missions, Venus surface sample return, Mars sample return	>150 W/kg specific power Operate to 5 AU	50–100 W/kg Unknown LILT effect
Electrostatically clean arrays	Sun Earth connection missions	<120% of the cost of a conventional array	~300% of the cost of a conventional array
Mars arrays	Mars smart lander, Mars sample return, scout missions	26% efficiency >180 sols @ 90% of full power	24% 90 sols @ 80% of full power
High-temperature solar arrays	Solar probe, sentinels	≥350°C operation (higher temperatures reduce risk and enhance missions)	130°C steady state; 260°C for short periods
High-efficiency cells	All missions	30+%	27%
Low intensity low temperature (LILT), resistant arrays	Outer planet missions, SEP missions	No insidious reduction of power under LILT conditions	Uncertain behavior of MJ cells under LILT conditions
High-radiation missions	Europa and Jupiter missions	Radiation resistance with minimal weight and risk penalty	Thick cover glass

Table 10.3 Measured global AM1.5 and measured or [a]estimated AM0 efficiencies for small-area cells

Cells	Efficiency [%] Global AM1.5	Efficiency [%] AM0	Area [cm^2]	Manufacturer
c-Si	22.3	21.1	21.45	Sunpower [17]
Poly-Si	18.6	17.1[a]	1.0	Georgia Tech/HEM [18]
c-Si film	16.6	14.8[a]	0.98	Astropower [19]
GaAs	25.1	22.1[a]	3.91	Kopin [19]
InP	21.9	19.3[a]	4.02	Spire [19]
GaInP (1.88 ev)	14.7	13.5	1.0	ISE [18]
GaInP/GaAs/Ge	31.0	29.3	0.25	Spectrolab [20]
$Cu(Ga,In)Se_2$	18.8	16.4[a]	1.04	NREL [19]
CdTe	16.4	14.7[a]	1.131	NREL [19]
a-Si/a-Si/a-SiGe	13.5	12.0	0.27	USSC [19]
Dye-sensitized	10.6	9.8[a]	0.25	EPFL [19]

[a]Estimated AM0 efficiencies based on cells measured under standard conditions. The calculated efficiency used the ASTM E490-2000 reference spectrum and assumes that the fill factor does not change for the increased photocurrent. Quantum efficiencies corresponding to the table entries were used in the calculations

(although, low-energy protons can cause problems in the unshielded gap areas on the front of solar cells and on the unshielded back). Ionization effects can reduce the transmittance of the solar cell cover glasses through the development of color centers. Ionized electrons caused by the radiation become trapped by impurity atoms in the oxide to form

stable defect complexes. Ionizing radiation is also a large detriment to the other materials associated with space solar arrays. It causes trapped charges to be created in silicon dioxide passivating layers that can lead to increased leakage currents. Ionizing radiation, including ultraviolet photons, is particularity bad for organic materials such as polymers used in array development as it can produce ions, free electrons, and free radicals that can dramatically change the optical, electrical, and mechanical properties of these materials.

The loss of energy of the high-energy protons and electrons due to interactions with electrons in a material accounts for a large fraction of the dissipated energy. In fact, these collisions are used to determine the penetration range for the electrons and protons in the 0.1 to 10 MeV range. However, it is the atomic displacements created by irradiation that are the major cause of degradation in space solar cells.

The displacement of an atom from a lattice site requires energy similar to that necessary to sublime an atom or to create a vacancy. The energy of sublimation for Si is 4.9 eV and for vacancy formation is 2.3 eV. The displacement of an atom requires the formation of a vacancy, an interstitial, and usually the creation of some phonons. Therefore, to create a displacement will require energy several times larger than that to create a vacancy.

The main importance of displacement defects due to irradiation is their effect on minority carrier lifetime. The lifetime in the bulk p-type material of a Si solar cell is the major radiation-sensitive parameter. This was the basis for the switch from p-on-n to n-on-p Si solar cells in the 1960s [21]. The minority carrier lifetime or diffusion length in an irradiated solar cell may be a function of excess or nonequilibrium minority carriers. This behavior is referred to as injection level dependence. This is usually associated with damage due to high-energy protons.

The primary radiation defects in Si are highly mobile. The radiation damage effects in Si are primarily due to the interaction of primary defects with themselves and with impurities in the material. Radiation damage in these cells can be mitigated to a certain extent by removing some of the damage before it becomes consolidated. Radiation-resistant Si cells use intrinsic gettering to remove a part of the radiation damage while it is still mobile. These cells contain a relatively pure region near the surface or "denuded zone" with a gettering zone rich in oxygen deeper in the wafer away from the junction. Although this approach decreases the beginning-of-life (BOL) output, it increases the end-of-life (EOL) output. The cells are much more radiation-resistant, which can dramatically extend the mission lifetime.

Annealing of irradiated solar cells can be used to remove some of the damage, although not at temperatures that would be considered practical for space applications. Temperatures of nearly 400°C are required for significant improvement in Si cells. However, there is some amount of ambient annealing of radiation damage that can occur. In space the damage and annealing process are occurring simultaneously and are thus hard to quantify. However, in the lab, ambient annealing improvement of as much as 20% in the short-circuit current has been observed after 22 months.

The main method for mitigating radiation damage in space solar cells is to prevent damage by employing a cover glass. The cover glass not only stops the low-energy protons but also slows down the high-energy particles. It can also serve to stop micrometeors,

act as an antireflection coating, provide resistance to charging, and even provide added thermal control to the spacecraft. In the 1970s, manufacturers began adding a nominal 5% cerium oxide to the cover glasses. This was shown to significantly improve the resistance of the glass to darkening from radiation or ultraviolet light [22]. The protection offered by the cerium also will improve the lifetime of the adhesives that are used to bond the cover glasses. The SOA cover glass is a drawn cerium-doped borosilicate glass. Research today is focused on improving the transmission of the glasses over a wider spectral range to accommodate the development of new MJ devices.

Current methods for calculating damage to solar cells are well documented in the GaAs Solar Cell Radiation Handbook (JPL 96-9). Recently the displacement damage dose (Dd) method has been developed to model radiation degradation. This method is currently being implemented in the SAVANT radiation degradation modeling computer program [23].

The bombardment of cells by charged particles can also lead to dangerously high voltages being established across solar arrays. These large voltages can lead to catastrophic electrostatic discharging events. This is especially true in the case of large arrays and pose significant problems for future utilization of large-area arrays on polymeric substrates. Much work has been done on the grounding and shielding of arrays to mitigate the effects of array charging [24]. Progress in addressing these effects has been made through the development of plasma contactors that ground the arrays to the space plasma.

Solar cell performance is also diminished over time due to neutral particle or micrometeor bombardment. These events account for approximately a 1% decrease in EOL space solar cells performance [25]. These events may also have a correlation to the initiation of discharging events discussed above. Space solar cells and arrays must also be equipped to contend with the plasma environment (radiation and charging). Removed from much of the shielding effects of the Earth's magnetic field, solar cells in space are continually bombarded with high-energy electrons and protons. The radiation damage caused by these particles will degrade solar cell performance and can dramatically limit spacecraft life. This is especially true for mid-Earth orbits (MEO, defined as $\sim$2000 to 12 000 km) in which cells must pass through the Van Allen radiation belts and thus get a much higher dose of radiation than would be experienced in low-Earth orbits (LEO, defined as $<$1000 km) or geosynchronous Earth orbits (GEO, defined as 35 780 km). LEO orbits vary in their radiation dose depending on their orientation, with, for example, polar orbits yielding a higher radiation dose than equatorial orbits. Figure 10.3 shows a comparison of equivalent fluence on a silicon solar cell in a variety of orbits. Figure 10.4 shows the dramatic decline in EOL power of cells in MEO orbit [26]. The degradation of cells in space due to radiation damage can be mitigated through the use of cover glasses at the expense of added mass to the spacecraft. Figure 10.5 shows the decline in power density as a function of time over 10 years in an 1853-km, 103° sun-synchronous orbit.

10.2.2 Thermal Environment

There is a considerable range of temperatures and intensities that may be encountered for the space use of photovoltaics. The temperature of a solar cell in space is largely determined by the intensity and duration of its illumination [32]. In a typical LEO, such as the orbit of the ISS, the operating temperature of the silicon solar cells is 55°C when

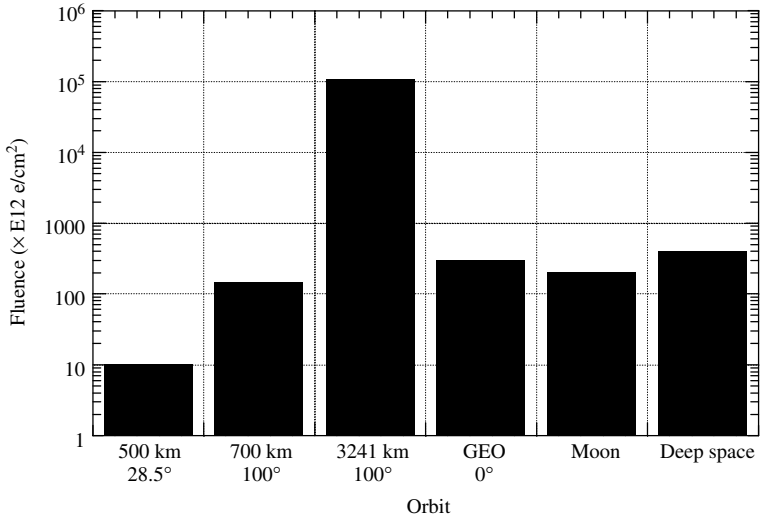

Figure 10.3 Equivalent 1-MeV electron fluence for a silicon solar cell in a variety of orbits (altitude in kilometer) and inclinations (°)

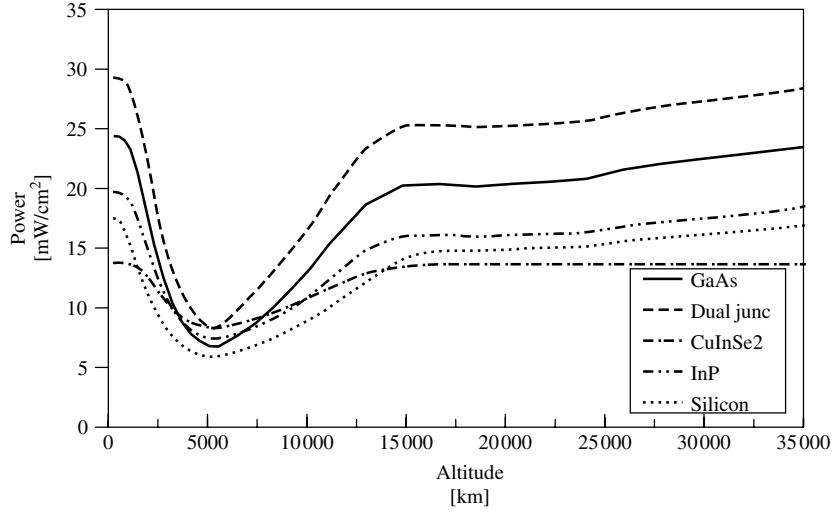

Figure 10.4 Solar cell power density as a function of altitude after 10 years in a 60° orbit with a cover glass thickness of 300 μm (GaAs: BOL 24.4 (mW/cm^2) [27]; Dual Junc – GaInP/GaAs/Ge [28]: BOL 29.3 (mW/cm^2); CuInSe2: BOL 14.4 (mW/cm^2) [29]; InP: BOL 19.7 (mW/cm^2) [30]; Si: BOL 17.5 (mW/cm^2) [31]). (Graph courtesy of Tom Morton, Ohio Aerospace Institute)

sun tracking and −80°C when in the longest eclipse. The average illuminated temperature at the orbit of Jupiter is −125°C, whereas at the average orbit of Mercury the temperature is 140°C. Similarly, the average intensity at the orbit of Jupiter is only 3% of the solar intensity at the Earth's radius, whereas the average intensity at Mercury is nearly double

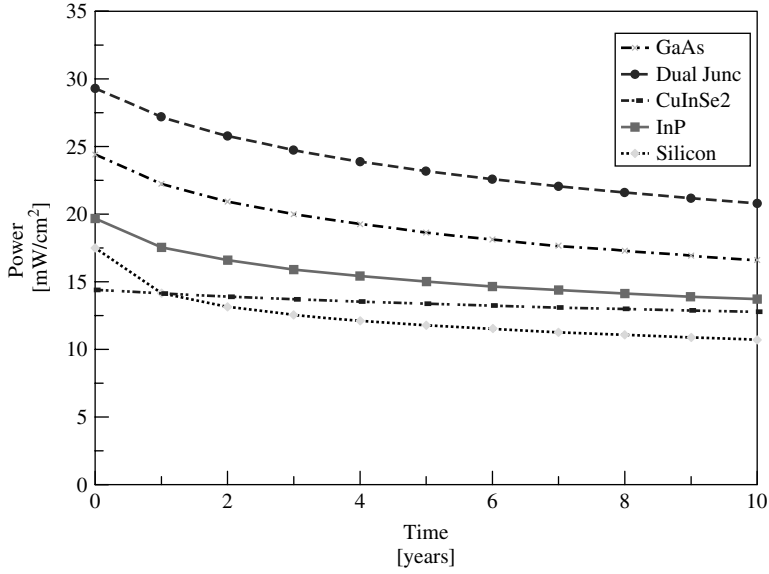

Figure 10.5 Solar cell power density as a function of time in a 1853-km altitude, 103° sun-synchronous orbit for the same cells as in Figure 10.6. (Graph courtesy of Tom Morton, Ohio Aerospace Institute)

that at Earth. The solar intensity in the orbit around the Earth will vary seasonally because of the ellipticity of the Earth's orbit around the sun. Orbital characteristics are also a major source of thermal variation. Most spacecraft experience some amount of eclipse that will vary as the orbit precesses. This can result in very large and rapid temperature changes as shown above for the space station cell. The temperature of a solar cell in space is also affected by the fraction of incident solar radiation returned from a planet or albedo. The average albedo from the Earth is 0.34, but can range anywhere from 0.03 (over forests) to 0.8 (over clouds) [7]. Typically, the range of temperatures experienced by solar cells in orbit about the Earth is from about 20°C to as high as 85°C.

An increase in solar cell temperature will cause a slight increase in the short-circuit current but a significant decrease in the open-circuit voltage (see Figure 10.6). Therefore, the overall effect is a reduction in power of a solar cell with an increase in temperature. It is typically less than 0.1%/°C, but can vary dramatically depending on cell type. This change coupled with rapid changes in temperature associated with eclipses can result in power surges that may be problematic.

The degradation of solar cell performance as a function of temperature is expressed in terms of temperature coefficients. There are several different temperature coefficients used to describe the thermal behavior of solar cells. These coefficients are generally expressed as the difference in a device parameter (i.e. I_{SC}, V_{OC}, I_{mp}, V_{mp}, or η) measured at a desired temperature and at a reference temperature [traditionally 28°C, although the new International Space Organization (ISO) standard is 25°C] divided by the difference in the two temperatures. Solar cell response to temperature is fairly linear for most cells over the range of −100 to 100°C. Unfortunately, for cells of amorphous silicon or low

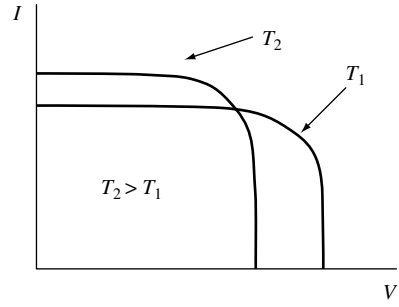

Figure 10.6 Effect of increasing temperature on solar cell $I-V$ photoresponse

Table 10.4 Theoretical normalized efficiency temperature coefficients [33]

Cell type	Temperature [°C]	η (28°C)	$(1/\eta)(d\eta/dT)$ [$\times 10^{-3}$/°C]
Si (calc.)	27	0.247	−3.27
Ge (calc.)	27	0.106	−9.53
GaAs (calc.)	27	0.277	−2.4

Table 10.5 Measured temperature coefficients for various types of solar cells used in space [26]

Cell type	Temp [°C]	η (28°C)	$(1/\eta)(d\eta/dT)$ [$\times 10^{-3}$/°C]
Si	28–60	0.148	−4.60
Ge	20–80	0.090	−10.1
GaAs/Ge	20–120	0.174	−1.60
2-j GaAs/Ge	35–100	0.194	−2.85
InP	0–150	0.195	−1.59
a-Si	0–40	0.066	−1.11 (nonlinear)
$CuInSe_2$	−40–80	0.087	−6.52

band gap cells such as InGaAs, the response is only linear with temperature for small temperature differences. Another frequently used definition for the temperature coefficient is the normalized temperature coefficient. In the case of the efficiency it is defined as

$$\beta = \frac{1}{\eta}\frac{d\eta}{dT} \tag{10.1}$$

or the fractional change in efficiency with temperature. Theoretical values for the normalized efficiency temperature coefficients for Si, Ge, and GaAs are given in Table 10.4. Representative temperature coefficients for the various types of cells used in space are given in Table 10.5. In general, the temperature coefficient decreases in magnitude with the increasing band gap but is always negative except in the case of a-Si, which can have a positive coefficient.

10.2.3 Solar Cell Calibration and Measurement

Calibration of solar cells for space is extremely important for satellite power system design. Accurate prediction of solar cell performance is critical to solar array sizing, often required to be within 1%. Calibration standards as a function of band gap are required to perform simulated AM0 efficiency measurements on earth. The calibration standards are produced by evaluating various cell types in space via the Shuttle or in the near future aboard the ISS. A less-costly means of developing standards is through the use of high-altitude aircraft or balloon flights. NASA Glenn Research Center solar cell calibration airplane facility has been in operation since 1963 with 531 flights to date [34]. The calibration includes real data to AM0.2 and uses the Langley plot method plus an ozone correction factor to extrapolate to AM0. Comparison of the AM0 calibration data indicates that there is good correlation with Balloon and Shuttle flown solar cells.

Solar intensity is a function of the thickness of the atmosphere that the sunlight must pass through (AM). Plotting the logarithm of solar cell short-circuit current, proportional to solar intensity, as a function of AM permits extrapolation to an unmeasured AM and AM0 (Langley Plot Method). Early ground-based measurements were based on the change in atmosphere that the sun would pass through as it moves across the sky (i.e. more atmosphere at dawn and dusk and a minimum at solar noon). This is the same basic method that is used with an airplane, changing altitude to vary the AM.

Data analysis from early flights between 1963 and 1967 showed that the AM0 extrapolation was slightly lower than what was expected from radiometer data. This was found to be due to ozone absorption of sunlight in the upper atmosphere. A change in the data linearity was also noticed when the plane flew below the tropopause. This was later correlated with Mie scattering from particulate matter in the atmosphere and with absorption by moisture. These effects are primarily manifested in the higher-energy region of the solar spectrum. Calibration flights currently are performed above the troposphere and a correction for ozone absorption is used. Today calibration runs are performed with a Lear 25A jet housed at the NASA Glenn Research Center (see Figure 10.7). It has flown 324 flights since 1984. The plane can fly up to $\sim$15 km and gets above AM0.2 at 45°N latitude. The data is now gathered using a continuous descent rather than remaining level over a range of altitudes.

The current Lear test setup has a 5:1 collimating tube in place of one of the original aircraft windows. This tube illuminates a 10.4-cm-diameter temperature-controlled plate. The tube angle can be adjusted to the sun angle. During descent IV curves for up to 6 cells, a pressure transducer, a thermopile, and a temperature sensor are all measured. The cells are held at a constant temperature of $\pm 1^{\circ}$C. A fiber optic connected to the test-plate is also connected to a spectroradiometer that can measure the solar spectrum from 250 to 2500 nm with 6-nm resolution, and a second spectrometer is used to measure the spectrum from 200 to 800 nm with 1-nm resolution. Both of these spectrometers are used to check for any spectral anomalies and to provide information on the ozone absorption.

There are currently several commercially available steady-state and pulse solar simulators that can simulate the sun's light in a variety of conditions (i.e. AM1.5, AM0). The NASA Glenn Research Center uses a Spectrolab X-25 Mark II xenon arc-lamp solar simulator. Steady-state solar simulators are generally used in laboratory or production environments for precision testing of PV devices. Solar simulators are also used on

Figure 10.7 The NASA Glenn Research solar cell calibration aircraft. (Photo courtesy of NASA)

terrestrial, aerospace, and satellite products as a long-term simulated sunlight exposure system to test optical coatings, thermal control coatings, paints, and so on. Pulse simulators make it possible to test large solar cell assemblies and solar array blankets.

NASA Glenn uses a Spectrolab Spectrosum Large Area Pulsed Solar Simulator. It has a xenon arc lamp that is flashed to produce approximately 1-sun illumination with a nearly AM0 spectrum. The flash lasts approximately 2 ms, during which time the voltage across the cell is ramped and the resulting current is measured. At the same time the short-circuit current from a standard solar cell of a similar type is used to adjust the measured test sample current for the slightly changing illumination during the flash.

The standards for space solar cell calibration fall under the auspices of the ISO technical committee 20: Aircraft and Space Vehicle, sub committee 14: Space Systems and Operation. The working draft ISO 15387 addresses the requirements for reference solar cells, the extraterrestrial solar spectral irradiance, and the testing conditions. Round robin testing procedures, which rotate the cell measurements from agency to agency, involving NASA, CAST, and ESA for space solar cell calibration are currently under way.

10.3 SILICON SOLAR CELLS

Silicon solar cells are the most mature of all space solar cell technologies and have been used on practically every near-Earth spacecraft since the beginning of the US space program. In the early 1960s, silicon solar cells were ~11% efficient, relatively inexpensive, and well suited for the low-power (100 s of watts) and short mission duration (3–5 years). The conversion efficiency of current "standard-technology" silicon ranges from around 12 to 15% under standard AM0 test conditions [19]. The lower efficiency cells are generally more resistant to radiation.

Cell efficiencies for any application should be adjusted for the array packing factor, radiation damage, ultraviolet degradation, assembly losses, and for corrections due to variations in intensity and temperature from standard conditions. At operating temperature, a silicon solar cell will degrade about 25% over 10 years in GEO orbit owing to charged

particle irradiation damage [35]. The performance of these cells degrades significantly (often exceeding a 50% loss) in very high-radiation environments such as experienced near Jupiter or in MEO. The relatively large temperature coefficient of silicon cells also results in large reductions in efficiency at high temperatures [26].

There have been many enhancements to silicon cells over the years to improve their efficiency and make them more suitable to space utilization. Textured front surfaces for better light absorption, extremely thin cells with back surface reflectors for internal light trapping, and passivated cell surfaces to reduce losses due to recombination effects are just a few examples and are discussed in more detail in Chapters 7 and 8. Currently, high-efficiency Si (HES) cells approaching 17% AM0 efficiency in production lots are available from several producers. The advantage of the HES cell to that of a III-V lies in their relatively lower cost and lower material density. However, silicon solar cells are less tolerant of the radiation environment of space.

10.4 III-V SOLAR CELLS

The efficiency of space solar cells achieved dramatic improvements as the focus shifted from Si toward GaAs and III-V semiconductor systems. The 1.43 eV direct band gap is nearly ideal for solar conversion (see Figure 10.1). By 1980 several types of III-V cells had been tested in space, with a 16% GaAs solar cell being developed by 1984 and a 18.5% efficient GaAs/Ge solar cell developed by 1989. It was also found that the GaAs cells had significantly better radiation resistance than Si cells. GaAs cells with efficiencies in excess of 80% of their theoretical maximum were routinely available commercially by 1998. Single-junction GaAs on Ge cells are currently commercially available with an AM0 efficiency of 19% and V_{OC} of 0.9 V. III-V solar cells for space applications are currently grown on Ge wafers because of the lower cost and higher mechanical strength over GaAs wafers.

Investigations on further efficiency improvement toward the end of the 20th century turned toward the development of multiple-junction cells and concentrator cells. Much of the development of "multijunction" GaAs-based photovoltaics was supported by a cooperative program funded by the Air Force Manufacturing Technology (ManTech) program and Space Vehicles Directorate, the Space Missile Center, and NASA [36]. This work resulted in the development of a "dual-junction" cell that incorporates a high band gap GaInP cell grown on a GaAs low band gap cell. The 1.85-eV GaInP converts short wavelength photons and the GaAs converts the lower energy photons. Commercially available dual-junction GaInP/GaAs cells have an AM0 efficiency of 22% with a V_{OC} of 2.06 V. See Chapter 9 for a complete discussion of this type of solar cell.

The highest-efficiency solar cells currently available for space use are triple-junction cells consisting of GaInP, GaAs, and Ge. They are grown in series of connected layers and have been produced with a 26.9% efficiency with a V_{OC} of 2.26 V in production lots, with laboratory cells of 29% (see Figure 10.8). Emcore, Inc., Tecstar, Inc., and SpectroLab, Inc., currently produce cells that are commercially available in the 25 to 27% range. Hughes Space and Communications Company's HS601 and HS702 spacecraft currently use MJ technology as do most other contractors for their high-performance spacecraft.

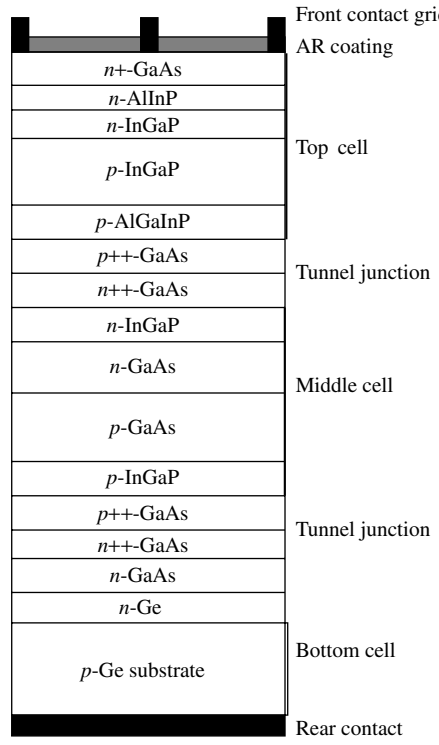

Figure 10.8 Commercially available 26.9% GaInP/GaAs/Ge triple-junction cell

Spectrolab, supplier of more than half of the world's spacecraft solar cells, has reached a milestone of 25 000 triple-junction GaInP/GaAs/Ge solar cells, with a maximum efficiency of 27.1% and an average conversion efficiency of 24.5%. They are currently providing 1 MW of cells to global spacecraft manufacturers (e.g. Hughes Space and Communication Company, Ball Aerospace & Technologies Group, Lockheed Martin, and Boeing). Their high-efficiency cells retain 86% of their original power after 15 years of operation. There is currently more than 50 kW of Spectrolab dual-junction solar cells in orbit.

The new multijunction III-V cells have allowed a reduction in solar array size and mass over the previously used Si cells while maintaining comparable power levels. The alternative way to view the efficiency increase offered by the III-V cells is that they have increased available payload power over using a comparably sized Si array. Scientists expect the majority of the 800 commercial and military spacecraft launched in the next five years to use multijunction III-V technology. This should result in the lower costs for telecommunications, Internet, television, and other wireless services. The AFRL recently initiated a 35% efficient four-junction solar cell program.

Multijunction III-V cells are relatively expensive to produce. The development of large-area arrays using these cells can become cost-prohibitive. One option to reduce the overall cost is to use the cells in solar concentrators, where a lens or mirror is used to decrease the required cell area. The previously mentioned SCARLET concentrator

arrays used on Deep Space 1 used GaInP/GaAs high-efficiency dual-junction cells. A more advanced SCARLET-II array will build on the SCARLET technology with lower cost, easier fabrication, and simplified assembly and testing [14].

10.4.1 Thin-film Solar Cells

One of the first thin-film cells, Cu_2S/CdS, was developed for space applications. Reliability issues eliminated work on this particular cell type for both space and terrestrial considerations even though AM1.5 efficiencies in excess of 10% were achieved. Thin-film cells require substantially less material and thus lower mass and promise the advantage of large-area, low-cost manufacturing. Until recently, the focus in space cells has been on efficiency rather than cost. In a several billion dollar spacecraft the solar cell cost is relatively small at even a thousand dollars per watt, which is approximately the current array cost. This has primarily been true for spacecraft with power needs from a few hundred watts to tens of kilowatts. However, deployment of a large Earth-orbiting space power system or some of the proposed SEP missions will require major advances in the PV array weight, stability in the space environment, efficiency, and ultimately the cost of production and deployment of such arrays. The development of viable thin-film arrays has become a necessity for a host of space missions [37]. Mission examples include ultra-long duration balloons (e.g. Olympus), deep space SEP "tug" array, Mars surface power outpost, and Mars SEP Array (see Figure 10.9). Solar electric propulsion missions are those in which the solar array is used to provide power for an electric propulsion system such as a Hall thruster or an ion thruster. These missions require large, lightweight, low-cost power systems. Studies have shown that the specific power or power per mass that will be required (i.e. 1 kW/kg) cannot be achieved with single-crystal technology [30]. The specific power required is almost 40 times what is presently available in commercial arrays. While high-efficiency ultralightweight arrays are not likely to become commercially available anytime soon, advances in thin-film photovoltaics may still impact other space technologies (i.e. thin-film integrated power supplies) and thus support a broad range of future missions.

Lighter power generation will allow more mass to be allocated to the balance-of-spacecraft (i.e. more payload). In addition, less expensive power generation will allow

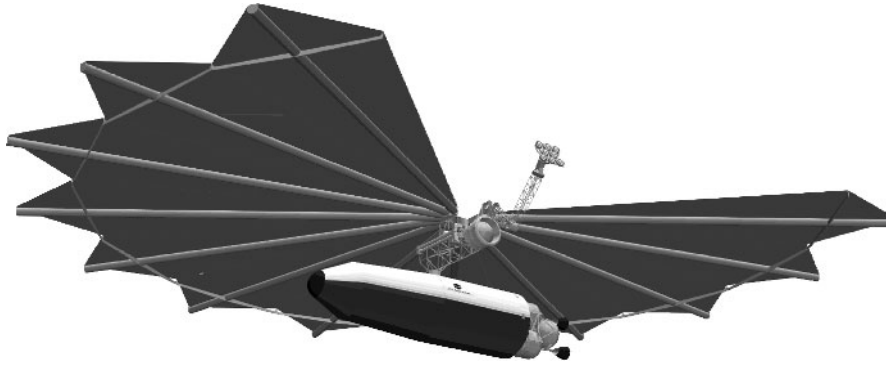

Figure 10.9 Proposed Mars solar electric propulsion vehicle. (Picture courtesy of NASA)

missions with smaller budgets and/or the allocation of funds to the balance-of-spacecraft. This is an essential attribute in enabling such missions as the Mars Outpost SEP Tug. An example of the benefits of thin-film PV arrays for the now-canceled ST4/Champollion indicates a $50 million launch cost savings and 30% mass margin increase when thin-film solar array power generation was combined with advanced electric propulsion. A parametric assessment showed similar advantages for other solar system missions (e.g. main belt asteroid tour, Mars SEP vehicle, Jupiter orbiter, Venus orbiter, Lunar surface power system) [30].

Much of the original development of thin-film PV arrays was performed with the terrestrial marketplace in mind. This has been a tremendous benefit to researchers hoping to develop such arrays for space. Features such as cell efficiency, material stability and compatibility, and low-cost and scalable manufacturing techniques are important to both environments. However, many key array aspects necessary for space utilization are not important for terrestrial use and thus have not experienced a similar progress. Features such as radiation tolerance, air mass zero (AM0) performance, use of lightweight flexible substrates, stowed volume and lightweight space deployment mechanisms must be developed before a viable space array can become a reality. Unfortunately, the costs associated with developing these features along with the subsequent space qualification studies mitigate the savings of using a thin-film array for space, and thus have inhibited their application.

On-going efforts by NASA and the U.S. Air Force are now addressing these issues associated with the development of thin-film arrays for space. Copper indium gallium diselenide (CIGS), cadmium telluride (CdTe), and amorphous silicon (a-Si) thin-film materials appear to have a good chance of meeting several proposed space power requirements [38]. Reasonably efficient (~8% AM1.5) large area flexible blankets using a-Si triple junction technology are already being manufactured.

Table 10.6 summarizes the thin-film solar cell technologies that are currently available. Further details on a-Si, CIGS, and CdTe solar cells can be found in Chapters 12–14, respectively. Several device structures offer specific power exceeding 1000 W/kg, but these values only include the device and substrate not the entire module and array. This table shows the importance of lighter or thinner substrates in achieving higher specific power. Note that multijunction cells (like the a-Si triple cells) whose thicknesses and bandgaps have been optimized for the terrestrial AM1.5 spectra should be re-optimized for AM0 since the distribution of photons between top, middle and bottom cells will be different. This changes the current matching. Reoptimization is not required for single junction thin-film devices. References 39 and 40 showed no substrate dependence for a-Si devices; that is, the same efficiency resulted between deposition on thin (10–25 μm) or thick (125 μm) stainless steel or between stainless steel or Kapton. This is good news for obtaining lighter thin film modules with higher specific power. In contrast, efficiency of Cu(InGa)S devices decreased from 10.4% to 4.1% as the stainless steel substrate decreased in thickness from 128 μm to 20 μm [44]. An 11% efficiency for CdTe on 10 μm polyimide was reported but is unpublished [45].

Development of other wide bandgap thin-film materials to be used in conjunction with CIGS to produce a dual-junction device is underway. As has already been demonstrated in III-V cells for space use, a substantial increase over a single-junction device

Table 10.6 Small area thin-film solar cell efficiency and specific power. AM0 and AM1.5 given when available. Results for a-Si devices in initial state before stabilization. AM0 results for a-Si triple junctions of a-Si/a-SiGe/a-SiGe [42] are higher than AM1.5 because they were optimized for AM0 spectrum, all other cells optimized for AM1.5. Substrate thickness estimated in some cases. Specific power calculated by authors with some assumptions. (n/a means not available)

Cell type	Cell + substrate thickness	AM1.5 efficiency [%]	AM0 efficiency [%]	Specific power [W/kg] @AM1.5	Reference for cell results
a-Si triple junction	Stainless steel, 128 μm	11.9	12.7	108	[39]
a-Si triple junction	Stainless steel, 7 μm	6.5	n/a	1080	[40]
a-Si triple junction	Kapton, 52 μm	~12 (est.)	12.7	~1200	[39]
a-Si double junction	Glass, ~1.5 mm	11.7	n/a	31	[41]
Cu(InGa)Se_2	Glass, ~1.5 mm	18.8	n/a	50	[42]
Cu(InGa)Se_2	Stainless steel 128 μm	17.4	n/a	156	[42]
Cu(InGa)Se_2	Polyimide 54 μm	12.1	n/a	1260	[43]
Cu(InGa)S_2	Stainless steel 128 μm	10.4	8.8	93	[44]
CdTe	Polyimide 10 μm	8.6	n/a	n/a	[45]
CdTe	Glass, ~1.5 mm	15	n/a	40	[46]

efficiency is possible with a dual-junction device. NASA and NREL have both initiated dual-junction CIS-based thin-film device programs. The use of Ga to widen the bandgap of CIGS and thus improve the efficiency is well established [42]. The substitution of S for Se also appears to be attractive as a top cell material. In particular, AM0 cell efficiencies 8.8% have been measured for $CuIn_{0.7}Ga_{0.3}S_2$ (E_g 1.55 eV) thin-film devices on flexible stainless steel substrates [44]. Other wide bandgap top cell possibilities under investigation include adding CdZnTe absorbers as discussed at the end of Chapter 14 .

The majority of thin-film devices developed for terrestrial applications have been on heavy substrates such as glass. However, progress is being made in reducing substrate mass through the use of thin metal foils and lightweight flexible polyimide or plastic substrates [47]. The use of such plastic substrates as Upilex or Kapton puts a slight restriction on the processing temperatures. This of course can be obviated by the use of metal foil if one is willing to accept the mass penalty.

In addition to cost and weight savings for spacecraft, thin-film solar cells have potential for improved radiation resistance relative to single-crystal cells, possibly extending mission lifetimes. For example, after a dose of 10^{16} 1 MeV *electrons*/cm^2, the maximum power generated by a GaAs cell can decrease to less than half of its BOL value. By contrast, after a dose of 10^{13}/cm^2 10 MeV *protons* (which would degrade GaAs cell power performance to less than 50% of BOL), the power generated by CIS cells has been shown to retain more than 85% of its BOL value [48].

In addition to thin-film cell development, there is the problem of making thin-film arrays for space. The flexibility of a thin-film cell on a polymeric substrate is a great advantage when it comes to stowability and deployment; however, it must be rigidly

supported after deployment. Work must be done to determine how best to deploy and maintain thin-film arrays. The same issues concerning stability in the space environment that were addressed for arrays with crystalline cells must now be addressed for thin-film arrays. As outlined in US Government Military Standard 1540C, the array must pass a number of qualification tests, including those for integrity and performance after exposure to elevated temperatures, radiation (particularly electrons and protons), thermal cycling, vibration and mechanical stress, and atomic oxygen.

The Air Force is leading a large, multidisciplinary team under the auspices of the Air Force Dual-Use Science and Technology program to develop a functional thin-film array for space within three years [49]. This program has the specific goals of demonstrating

1. a stabilized 10 to 15% AM0 efficient thin-film submodule;
2. submodule and module electrical architectures including bypass and blocking diode technology;
3. submodule and module mechanical interface architectures, module strength, and structural support requirements;
4. array support structure design for an array with a wide range of power levels;
5. space environment and thermal control protection/qualification standards for thin-film arrays.

This effort will culminate in the design of a-1 kW LEO and 20-kW GEO thin-film solar array.

10.5 SPACE SOLAR ARRAYS

Solar array designs have undergone a steady evolution since the Vanguard 1 satellite. Early satellites used silicon solar cells on honeycomb panels that were body-mounted to the spacecraft. Early space solar arrays only produced a few hundred watts of power. However, satellites today require low-mass solar arrays that produce several kilowatts of power. Several new solar array structures have been developed over the past 40 years to improve the array specific power and reduce the stowed volume during launch.

The most important characteristics of solar arrays required for space applications are

- high specific power (W/kg)
- low stowed volume (W/m^3)
- low cost ($/W)
- high reliability.

In addition, several proposed space missions have put other constraints on the solar arrays. Several proposed Earth-orbiting missions designed to study the sun require "electrostatically clean" arrays. Inner planetary missions and mission to study the sun within a few solar radii require solar arrays capable of withstanding temperatures above 450°C and functioning at high solar intensities (HIHT). Outer planetary missions require solar arrays that can function at low solar intensities and low temperatures (LILT). In addition to the near-sun missions, missions to Jupiter and its moons also require solar arrays that can withstand high-radiation levels.

The EOL power generated by an array is impacted in a variety of ways. Radiation damage will result in an 8% loss of BOL power/m^2 after 5×10^{14} 1 MeV electrons (i.e. typical EOL fluence in geosynchronous orbit). The temperature correction due to the operation of the solar cell at 75°C rather than at the 25°C test conditions will reduce the power/m^2 by ~9%. Degradation due to UV exposure is around 1.7%. Loss in power over time due to micrometeors and ordinary surface contamination are each around 1% [24].

The solar arrays presently in use can be classified into six categories:

- Body-mounted arrays
- Rigid panel planar arrays
- Flexible panel array
- Flexible roll-out arrays
- Concentrator arrays
- High-temperature/intensity arrays
- Electrostatically clean arrays.

A summary of the important typical characteristics of these arrays are given in Table 10.7.

10.5.1 Body-mounted Arrays

Body-mounted arrays are preferred for small satellites that only need a few hundred watts. Early spherical satellites and spin-stabilized cylindrical satellites used body-mounted arrays of silicon solar cells on the honeycomb panels. This type of array is simple and has proven to be extremely reliable. One of the limitations of this type of array is that it puts a constraint on the direction the spacecraft must point. This type of array is still used on smaller spacecraft and spin-stabilized spacecraft. The recently deployed Mars Pathfinder Sojourner Rover also used body-mounted solar arrays (see Figure 10.10).

10.5.2 Rigid Panel Planar Arrays

Rigid panel arrays have been used on many spacecraft requiring several hundred watts to many tens of kilowatts of power. They consist of rigid honeycomb core panels that

Table 10.7 Space solar array characteristics [16]

Technology	Specific power [W/kg] (BOL) @ cell efficiency	Cost [$K/W]	Area per power [m^2/kW]
High-efficiency silicon (HES) rigid panel	58.5 @ 19%	0.5–1.5	4.45
HES flexible array	114 @ 19%	1.0–2.0	5.12
Triple junction (TJ) GaAs rigid	70 @ 26.8%	0.5–1.5	3.12
TJ GaAs ultraflex	115 @ 26.8%	1.0–2.0	3.62
CIGS thin film[a]	275 @ 11%	0.1–0.3	7.37
Amorphous-Si MJ/thin film[a]	353 @ 14%	0.05–0.3	5.73

[a]Represents projected values. These arrays are unavailable commercially

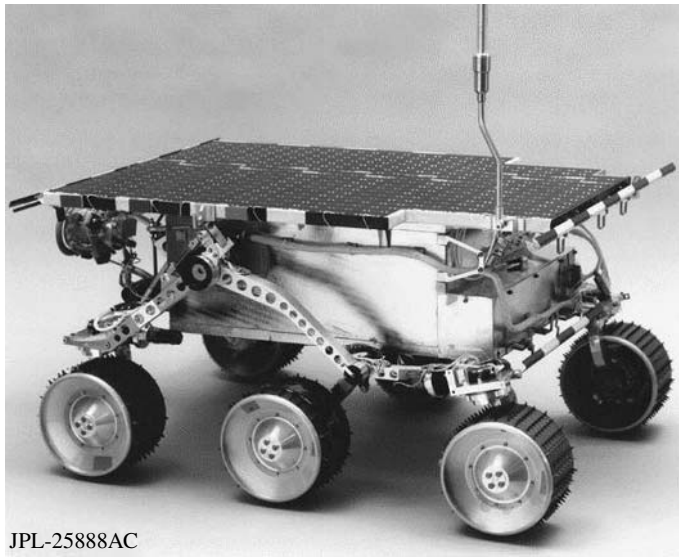

Figure 10.10 Body-mounted array on the Mars sojourner rover. (Picture courtesy of NASA JPL)

are hinged such that they can be folded against the side of the spacecraft during launch (see Figure 10.11). Each panel is rigid and quite strong, but can add considerably to the overall weight of the array. There has been much development recently on panels of materials other than aluminum (i.e. graphite/epoxy sheets and ribbons). Hybrid panels with aluminum honeycombs and epoxy/glass face sheets have also been developed. The folded arrays are deployed by means of pyrotechnic, paraffin, or knife blade actuators and damper-controlled springs.

The BOL power density of the rigid panel array is extremely dependent on the type of solar cell used. BOL power densities range from 35 to 65 W/kg for silicon cells and 45 to 75 W/kg for GaAs/Ge cells. The panel assembly of a rigid array accounts for 75 to 80% of the total mass, with the stowed and deployment structure making up the balance [16]. The Tropical Rainfall Measuring Mission (TRMM) and Rossi X-Ray Timing Explorer (XTE) both employ rigid panel arrays. Available power supplied by typical rigid panel arrays range from very small to in excess of 100 kW.

10.5.3 Flexible Fold-out Arrays

Flexible fold-out arrays are attractive for missions that require several kilowatts of power because of their high specific power, high packaging efficiency (low stowed volume), and simple deployment system. These arrays are generally designed in two basic configurations:

1. Flexible flat panel array with linear deployment as shown in Figure 10.12.
2. Flexible round panel array with circular deployment as shown in Figure 10.13.

These arrays have flexible or semiflexible panels that are stowed for launch with accordion folds between each panel. On reaching an appropriate orbit, these are unfurled

Figure 10.11 Rigid panel GaAs solar array (Picture courtesy of NASA). (The PV array is the two rectangular panels of five modules each)

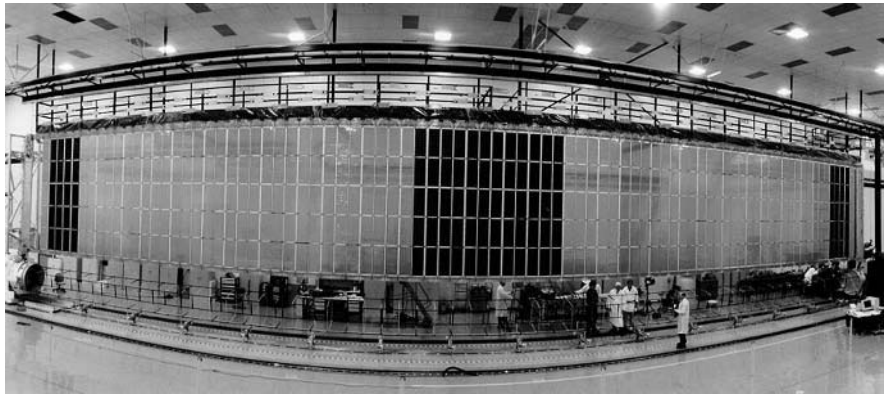

Figure 10.12 ISS array with linear deployment. (Figure courtesy of NASA)

by means of an Astromast™, an Ablemast™, or some other similar device. The specific power of these types of arrays varies from 40 to 100 W/kg, depending on the cell type, power, mission-reliability requirements, spacecraft orientation and maneuverability capabilities, and safety requirements. Initially, they were marketed as a significant improvement in power produced per unit mass. However, even though flexible arrays have an excellent figure-of-merit in this regard, the best rigid honeycomb panels have thus far matched their specific power performance. Very large flexible blanket solar arrays present complex structural and spacecraft design issues. This type of array is used on the MILSTAR series of spacecraft, on the TERRA spacecraft, and on the ISS (see Figure 10.2).

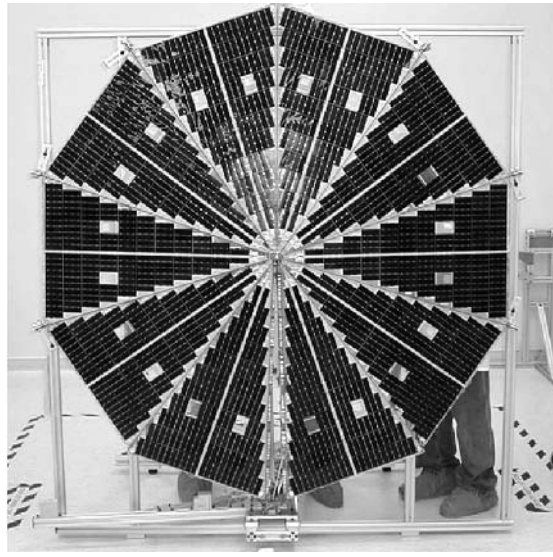

Figure 10.13 Flexible round panel array with circular deployment. (Picture courtesy of AEC-ABLE)

TRW, Inc., developed a flexible flat panel/rectangular array in the late 1980s, known as the Advanced Photovoltaic Solar Array (APSA), under a contract with NASA/JPL [50]. A similar array development was performed with DOD support. These arrays were based on the same fundamental concept of using polyimide panels stretched between lightweight hinges that could be deployed by an extendible mast. Silicon cells with an average AM0 efficiency of 14% were used for the arrays. The structure (mast, release motor, containment box) accounted for ~51% of the array mass with the panel assembly (polyimide substrate, solar cells, cover glass, and interconnect tabs, hinges, wiring harness) making up the balance.

The original APSA design was for 130 W/kg at 5.3 kW BOL in GEO. However, the specific power of this type of array does not scale linearly. The low-power arrays of this design had a specific power on the order of 40 to 60 W/kg. Projected BOL and EOL specific power of the APSA array for both Si and GaAs cells available in the early 1990s are given in Figure 10.14.

The Terra satellite uses an APSA-type array. The specific power of this array is only ~40 W/kg. This was due to the necessity of reinforcing the stowage box because the box could not be stiffened by the spacecraft structure as APSA had assumed. Also, a stronger and heavier substrate than that APSA had assumed would be possible was used. The ISS Array also had a BOL specific energy of 40 W/kg owing to additional maneuverability and safety and reliability requirements put on the arrays [13].

10.5.4 Thin-film or Flexible Roll-out Arrays

The flexible roll-out array is similar to the accordion-folded array mentioned earlier, except the fact that the semiflexible or flexible substrate is rolled onto cylinder for launch.

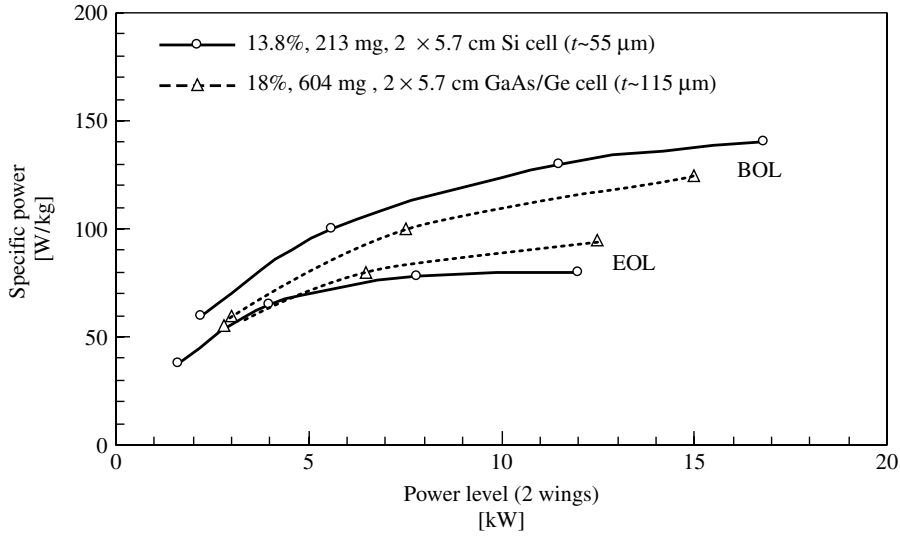

Figure 10.14 Projected specific power of the APSA array with various cell technologies [13]

The Hubble Space Telescope used such a roll-out array (see Figure 10.15). It contained a polyimide blanket in a roll-up stowed configuration. The array was deployed by a tubular, extendable boom (Bi-STEM) deployment system. The flexible role-out array design was developed for the US Air Force.

After eight years in orbit, the solar arrays on Hubble were replaced on orbit owing to degradation [51]. During the repair mission, delamination of the solar array bus bars was observed and it was also noticed that two of the hinge pins had started to creep out. One of the arrays was returned to Earth to be studied, while the other array was jettisoned into space. The returned solar array was shipped to ESA for further study. These roll-out arrays were replaced with rigid panels that were thought to be more reliable.

AFRL has begun a $6 M, three-year program with two prime contractors (Boeing and Lockheed Martin) to investigate and design complete arrays uniquely tailored to thin-film solar cells. The SquareRigger™ solar array being developed by AEC-ABLE is a flexible blanket system composed of modular "bays." This array is attempting to combine an ultra-high-power capability (>30 kW) with a high stowed packaging efficiency. The SquareRigger™ solar array system is projected to achieve a specific power between 180 to 260 W/kg BOL, depending on the type of cells used. A SquareRigger™ system using thin-film cells is projected to offer an order-of-magnitude reduction in cost over conventional rigid panel systems.

10.5.5 Concentrating Arrays

Photovoltaic concentrating arrays have been proposed for missions to outer planetary missions, solar electric propulsion missions, and missions that operate in high-radiation environments. These arrays are attractive for these missions because they have the potential to provide a high specific power, higher radiation tolerance, and improved performance in

Figure 10.15 Roll-out arrays used on the Hubble space telescope. (Photo courtesy of NASA)

LILT environments. The technical issues in using concentrating arrays are precision pointing, thermal dissipation, nonuniform illumination, optical contamination, environmental interactions, and complexity of deployment. They can also decrease overall spacecraft reliability because a loss of pointing may cause significant power loss to the spacecraft.

Reflective systems can have concentration ratios from 1.6X to over 1000X, with a practical limit of around 100X. Refractive designs are generally limited to the range of about 5X to 100X, with a practical limit of around 20X. Solar energy may be focused on a plane, line, or point depending on the geometry of the concentrator design. These concentrators may be small and numerous if used in a distributed focus design or they may be a single large concentrator as in a centralized focus design.

AstroEdge™ array on the NRO STEX spacecraft, launched in October 1998, was the first spacecraft to use a concentrator as its main power source. This system used a reflective trough design with a nominal 1.5X concentration. The arrays were successfully deployed and cell currents were slightly higher than predicted. Thermal problems did occur on some of the panels owing to the higher concentrator operating temperature.

The Deep Space 1 spacecraft launched in October 1998 used SCARLET concentrator arrays to provide power to its ion propulsion engines (see Figure 10.16) [14]. Its two arrays were capable of producing 2.5 kW at 100VDC. The Scarlet array was developed by AEC-ABLE under a program sponsored by BMDO.

The SCARLET array has a refractive linear distributed focus with a 7.5X concentration ratio. The array has 720 lenses to focus sunlight onto 3600 solar cells. Deep Space 1 has two SCARLET solar array wing assemblies. Each assembly is made up of a composite yoke standoff structure, four composite honeycomb panel assemblies, and four lens frame assemblies. High-efficiency triple-junction $GaInP_2$/GaAs/Ge cells were used in this array.

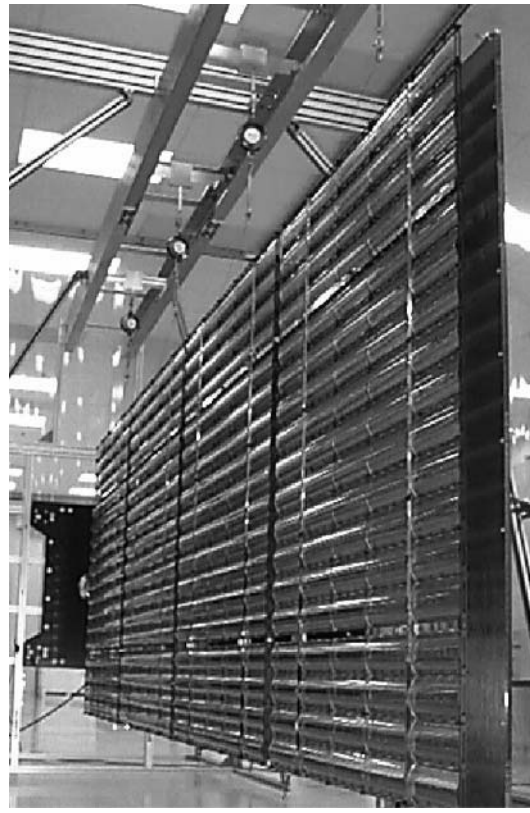

Figure 10.16 The SCARLET array used on Deep Space 1

The first commercial concentrator array developed for space was the Boeing 702. It was used on the Galaxy XI spacecraft and was deployed on January 12, 2000. It has a reflective planar centralized focus concentrator design in which the sun's rays are reflected onto a single rectangular plane of solar cells. It used thin-film reflectors and had a 1.7X concentration. It was designed for power levels of 7 to 17 kW over a 16+ year design life. The array deployed as expected and its initial power output was within the expected range. However, its concentrator surfaces degraded very quickly while in orbit. The specific power of this array was ~60 W/kg using 24% efficient MJ solar cells. The similar Boeing 601 bus, which uses an ordinary planar solar array, is limited to about 15 kW of power owing to the array stowed volume limitations.

10.5.6 High-temperature/Intensity Arrays

Missions to Mercury and other missions with close encounters to the sun (i.e. solar probe) have generated the need for cells and arrays that are capable of operating in high–light intensity, high-radiation, and high-temperature environments. Two missions that had to contend with such an environment have already flown. Helios A, which reached

0.31 Astronomical Units (AU) – the average Earth to sun distance – was launched on December 10, 1974 and Helios B, which reached 0.29 AU, was launched on January 15, 1976. These spacecraft used ordinary silicon cells that were modified for high-intensity use and had second surface mirrors to cool the array. The remainder of their technology was very similar to what is used on standard arrays. In addition to these missions, the upcoming MESSENGER Discovery mission is planned for travel to 0.31 AU. Its solar array design is already under development.

The current solar array technology can meet the needs of MESSENGER or other spacecraft that approach the sun to about 0.3 AU, but with reduced performance and increased risk compared to other applications. Further progress is required in both cell and array development for closer encounters to the sun. The common feature to the high-temperature and high-intensity solar arrays that have operated thus far is the replacement of a significant fraction of the solar cells by optical solar reflectors (OSRs). These are mirrors that help control the array temperature near the sun at the cost of reduced power at larger distances.

The MESSENGER design also off-points the array as the spacecraft nears the sun to keep the array below 130°C. The array is designed to tolerate pointing at the sun for a maximum of 1 h (probably much longer). However, it will be unable to function under this extreme condition (i.e. 260°C).

The US Air Force and BMDO also developed some high-temperature arrays in the late 1980s. The Survivable COncentrating Photovoltaic Array (SCOPA) and SUrvivable PowER System (SUPER) were designed to be capable of surviving laser attack. These were concentrator arrays that directed the incident laser light away from the solar cells. Although the laser light would not impinge directly, the arrays' temperature would increase dramatically and thus the arrays needed to withstand several hundred degrees Celsius.

The high-temperature survivability of SCOPA and SUPER was achieved through changes to the contact metallization and through the use of diffusion barriers in the GaAs cells used. Both Tecstar and Spectrolab developed the cells in conjunction with this effort. Other smaller companies such as Astropower, Kopin, and Spire have also worked on developing high-temperature cells. GaAs cells reaching an AM0 efficiency of 18% were produced that degraded less than 10% under one-sun after annealing in vacuum for 15 min at 550°C. Concentrator cells were produced that survived repeated 7-min excursions to 600°C. These same cells exhibited only 10% loss with exposure to 700°C. NASA is also currently funding an effort to develop wide band gap solar cells for high-temperature/high-intensity environments. Cells using materials such as SiC, GaN, and AlGaInP are being developed [52]. These cells may also benefit from high-emissivity selective coatings that will limit the unusable IR entering the solar cells and reduce their steady-state temperature.

10.5.7 Electrostatically Clean Arrays

There is an entire class of proposed missions designed to study the Sun–Earth Connection (SEC). These spacecraft typically measure the fields and particles associated with the solar wind. This requires that arrays be developed that do not distort the local environment

or be electrostatically "clean." These arrays must have their voltage separated from the space plasma and the array must be maintained at the same potential as the spacecraft. This is usually accomplished by coating the cell cover glass and arrays between the cells with a conductor. Since the coating for the cover glass must be transparent, a transparent conducting oxide (TCO) such as indium tin oxide is used. The coatings between the cells must not short them out, so an insulating coating must first be applied to all of the interconnects before the conductive coating or "v" clips. All of this must be done within a thickness of ~0.08 mm and within a width of about 0.8 mm.

Fabricating an electrostatically clean array presently costs three to six times as much as a typical array. This is due in large part to the hand labor involved in developing such arrays. These arrays are also less reliable due to the lack of robustness of the conductive coatings used to maintain the equipotential. In addition, these arrays are also generally body-mounted, which cuts down on the available power to the spacecraft (i.e. pointing issues, etc.). The power is also limited due to the thicker cover glass that is employed owing to the high-radiation environment associated with SEC missions. Unfortunately, there is not a wide knowledge base on how to develop electrostatically clean arrays. This was demonstrated in the cost of developing the Fast Auroral Snapshot (FAST) solar array. The electrostatically clean body-mounted solar panels for FAST cost in excess of $7400 per test condition watt.

The use of monolithic diodes on the latest generation of MJ solar cells could prove to be a tremendous advantage in developing electrostatically clean arrays. The presence of antennas, booms and outcroppings from a body-mounted array, requires that solar cells have bypass diodes to reduce the shadowing losses and potential damage to the arrays. The new built-in diodes will obviate the need and the expense involved in adding the diodes to the array circuitry. The NASA Goddard Space Flight Center (NASA-GSFC) recently funded Composited Optics Incorporated (COI) to study electrostatically clean arrays through the Solar Terrestrial Probe (STP) Program's Magnetospheric Multiscale (MMS) and Geospace Electrodynamic Connection (GEC) projects. COI will be supplying the electrostatically clean solar panels for the Communication/Navigation Outage Forecast System (CNOFS).

10.5.8 Mars Solar Arrays

Mars orbiters have used PV arrays that are quite similar to those used in Earth orbit with good results. However, Mars surface missions, in which the solar spectrum is depleted at short wavelengths, causes the efficiency of the cells to be lower than that if the cells were operated above the atmosphere of Mars. The cell efficiency is reduced by about 8% (relative %). In addition, the effect of dust accumulating on arrays was observed on the Mars Pathfinder mission by monitoring the J_{SC} of cells exposed to the environment whose short-circuit current could be monitored on a routine basis. One cell indicated an increase in obscuration of about 0.3%/sol for the first 20 sols (note that a "sol" is a Martian day of 24.6 h). The other cell indicated that over a longer period of ~80 sols, the obscuration flattened out and seemed to be approaching an asymptote of around 20% obscuration [53]. Cells that are "tuned" to the Martian solar spectrum and methods for mitigating dust obscuration will be necessary to produce efficient arrays for Mars surface power.

10.5.9 Power Management and Distribution (PMAD)

There are a number of different devices involved in efficiently connecting a space solar array to its intended loads. A system for managing and distributing the power consists of regulators, converters, charge controllers, blocking diodes, and wiring harness [54]. This system must condition the power to maintain the appropriate current and voltage levels to the power subsystems under varying illumination, temperature, and with cell degradation over the mission lifetime. The electrical bus for this system must also be able to isolate individual panel faults in such a way that the entire spacecraft will not loose total power in the case of a panel failure. The entire Power Management and Distribution (PMAD) typically will account for 20 to 30% of the entire power system mass in the case of a conventional array. This can be reduced if an unregulated system is used.

Very often solar power generation is combined with a battery storage element that can be used in eclipse. In order to provide the appropriate charging conditions for the batteries and to avoid overcharging and heating, peak-power tracking (PPT) or direct energy transfer (DET) are used. PPT controls the arrays, so they only produce the power levels required by means of a DC-DC converter in series with the array. Peak-power tracking is typical on missions that need less power at EOL. A PPT system uses about 5% of the power produced by the array. Systems using DET operate using the fixed voltage of the array and shunt the excess power through shunt resistors. The fixed voltage of the array is chosen to be close to the EOL maximum power point voltage. These systems generally have a higher EOL efficiency and therefore are used on longer missions.

On an unregulated bus with a battery storage component, the loads will experience whatever voltage is currently on the batteries. This can lead to a large swing in voltage (i.e. 20%) to the load depending on the battery chemistry and the depth of discharge. In a quasi-regulated system that employs a simple battery charger, the loads will be maintained at a voltage that is higher than the voltage on the batteries during charging. However, the loads will track the decrease in battery voltage as they are discharged (i.e. during eclipse). A fully regulated system that uses a regulator will maintain a constant load voltage independent of the charging or the discharging cycle. A fully regulated system requires more elements and thus increases the PMAD complexity and mass. There will also be a decrease in system efficiency due to the power loss from overall bus resistance. However, it does provide more reliability and increases battery life. The resistive power losses can be minimized by using a higher bus voltage. The maximum voltage limits on an array is set by the voltage that the exposed parts of the power system can hold off without discharging through the space plasma (i.e. $\sim$50 V for LEO).

10.6 FUTURE CELL AND ARRAY POSSIBILITIES

10.6.1 Low Intensity Low Temperature (LILT) Cells

The term LILT is used to refer to solar arrays operating under conditions encountered at distances greater than 1 AU from the sun. Typical Earth-orbiting solar arrays have steady-state illuminated temperatures of approximately 40 to 70°C. The efficiency of most cells increases down to about -50°C. This temperature would correspond to around

3 AU. Currently available solar cells have uncertain performance under LILT conditions. NASA Glenn Research Center has initiated a program to evaluate solar cells under LILT conditions and to look for ways of enhancing their performance.

10.6.2 Quantum Dot Solar Cells

A recent approach to increasing the efficiency of thin-film PV solar cells involve the incorporation of quantum dots [55]. Semiconductor quantum dots are currently a subject of great interest mainly due to their size-dependent electronic structures, in particular the increased band gap and therefore tunable optoelectronic properties. To date these nanostructures have been primarily limited to sensors, lasers, LEDs, and other optoelectronic devices. However, the unique properties of the size-dependent increase in oscillator strength due to the strong confinement exhibited in quantum dots and the blue shift in the band gap energy of quantum dots are properties that can be exploited for developing PV devices that offer advantages over conventional photovoltaics. Theoretical studies predict a potential efficiency of 63.2%, for a single size quantum dot, which is approximately a factor of 2 better than any SOA device available today. For the most general case, a system with an infinite number of sizes of quantum dots has the same theoretical efficiency as an infinite number of band gaps or 86.5%. See Chapter 4 for a more complete discussion of quantum dots and theoretical efficiencies.

A collection of different size quantum dots can be regarded as an array of semiconductors that are individually size-tuned for optimal absorption at their band gaps throughout the solar energy emission spectrum. This is in contrast with a bulk material in which all photons with $E > E_g$ are absorbed at the same energy, that is, the band gap. Their excess energy $E - E_g$ is wasted. In addition, bulk materials used in solar energy cells suffer from reflective losses at energies about the band gap, whereas for individual quantum dots reflective losses are minimized. Some recent work has shown that quantum dots may offer some additional radiation resistance and favorable temperature coefficients [56].

10.6.3 Integrated Power Systems

NASA has also been working to develop lightweight, integrated space power systems on small-area flexible substrates [57]. These systems generally consist of a high-efficiency thin-film solar cell, a high-energy density solid-state Li-ion battery, and the associated control electronics in a single monolithic package. These devices can be directly integrated into microelectronic or micro-electromechanical systems (MEMS) devices and are ideal for distributed power systems on satellites or even for the main power supply on a nanosatellite. These systems have the ability to produce constant power output throughout a varying or intermittent illumination schedule as would be experienced by a rotating satellite or "spinner" and by satellites in a LEO by combining both generation and storage.

An integrated thin-film power system has the potential to provide a low-mass and low-cost alternative to the current SOA power systems for small spacecraft. Integrated thin-film power supplies simplify spacecraft bus design and reduce losses incurred through energy transfer to and from conversion and storage devices. It is hoped that this simplification will also result in improved reliability.

The NASA Glenn Research Center has recently developed a microelectronic power supply for a space flight experiment in conjunction with the Project Starshine atmospheric research satellite (*http://www.azinet.com/starshine/*).

This device integrates a seven-junction small-area GaAs monolithically integrated photovoltaic module (MIM) with an all-polymer $LiNi_{0.8}Co_{0.2}O_2$ lithium-ion thin-film battery. The array output is matched to provide the necessary 4.2 V charging voltage, which minimizes the associated control electronic components. The use of the matched MIM and thin-film Li-ion battery storage maximizes the specific power and minimizes the necessary area and thickness of this microelectronic device. This power supply was designed to be surface-mounted to the Starshine 3 satellite, which was be ejected into a LEO with a fixed rotational velocity of 5° per second. The supply is designed to provide continuous power even with the intermittent illumination due to the satellite rotation and LEO [58].

10.6.4 High Specific Power Arrays

To achieve an array specific power of 1 kW/kg, a much higher cell specific power will be necessary. Similarly, the blanket specific power (i.e. interconnects, diodes, and wiring harnesses) must be over 1 kW/kg as well. The APSA assessment determined that the mass of the deployment mechanism and structure is essentially equal to the blanket mass for a lightweight system [21]. Therefore, a blanket specific power of approximately 2000 W/kg would be necessary to achieve a 1-kW/kg array. NASA is currently sponsoring an effort by AEC-ABLE Engineering to develop lightweight thin-film array deployment systems.

Gains in array specific power may be made by an increase in the operating voltage. Higher array operating voltages can be used to reduce the conductor mass. The APSA was designed for 28 V operation at several kilowatts output, with the wiring harness comprising ~10% of the total array mass, yielding a specific mass of ~0.7 kg/kW. If this array was designed for 300-V operation, it could easily allow a reduction of the harness specific mass by at least 50%. This alone would increase the APSA specific power by 5% or more without any other modification.

The extremely high specific power arrays that need to be developed for SEP and SSP applications will require lightweight solar arrays that are capable of high-voltage operation in the space plasma environment. SEP missions alone will require 1000 to 1500 V to directly power electric propulsion spacecraft (i.e. no voltage step-up is required to operate the thrusters). NASA has proposed a thin-film stand-alone array specific power that is 15 times the SOA III-V arrays, an area power density that is 1.5 times that of the SOA III-V arrays, and specific costs that are 15 times lower than the SOA III-V arrays [59].

10.6.5 High-radiation Environment Solar Arrays

There are several approaches to mitigating the effects of a high radiation on a solar array. The simplest is to employ thick cover glass (assuming that a commercial source could be developed). Thick cover glasses protect the cell from the highly damaging low-energy protons, but will cause a significant decrease in the specific power of the array. However, this can be reduced if one adopts a concentrator design, assuming of

course that the additional elements associated with the concentrator can withstand the high-radiation environment as well. A different approach is to try and develop cells that are more radiation-resistant. Several of the materials that are being investigated for high-temperature/high-intensity missions have also shown good radiation resistance. However, these will not be suited to the high-radiation missions involving LILT. Many of the high-radiation NASA missions being considered occur at distances much greater than 1 AU. Thin films may offer a possibility since they have demonstrated some advantages with regard to radiation tolerance as previously mentioned, provided the problem of their low efficiencies are solved.

10.7 POWER SYSTEM FIGURES OF MERIT

There are many figures of merit that must be considered in developing an SSP system (i.e. specific mass, specific power, cost per watt, temperature coefficients, and anticipated radiation degradation of the solar cells used).

The radiation hardness and the temperature coefficients for the III-V multijunction cells are significantly better than Si cells, as previously discussed. This leads to significantly higher EOL power level for a multijunction cell as compared to a Si cell. This is shown in Table 10.8, where the BOL cell efficiencies at room temperature and the typical EOL cell efficiencies for LEO and GEO operating temperatures and radiation environments are presented.

The difference in radiation degradation can have a huge impact on power system design. For example, if the area for a typical rigid panel is approximately 8 m^2 and the area of a typical solar cell is 24 cm^2, using a panel packing factor of 0.90 will allow the panel to have 3000 cells. Under GEO conditions, this panel populated with high-efficiency Si cells will produce 1.2 kW of EOL power. The EOL power could almost be doubled to 2.2 kW if it were populated with SOA triple-junction cells.

Table 10.8 A comparison of relative radiation degradation of 75-μm multijunction cells and high-efficiency Si under GEO and LEO operation [52]

Solar cell technology	BOL efficiency @ 28°C [%]	EOL efficiency on orbit [%]
GEO conditions (60°C) – 1-MeV, 5E14 e/cm²		
HE Si	14.1	12.5
2J III-V	20.9	20.0
3J III-V	23.9	22.6
LEO conditions (80°C) – 1-MeV, 1E15 e/cm²		
HE Si	13.4	10.6
2J III-V	19.7	18.1
3J III-V	22.6	20.3

Alternatively, the solar arrays populated with high-efficiency Si cells would need to be 77% larger than arrays using triple-junction cells in order to deliver the equivalent amount of EOL power in GEO and 92% larger in LEO.

The large difference in size between solar arrays populated with Si and MJ cells is very significant in terms of stowage, deployment, and spacecraft attitudinal control. This is especially true for very high-powered GEO communication satellites in which Si solar array area can exceed 100 m^2. The comparable array with triple-junction cells, although by no means small, would have an area of ~59 m^2. The array size will impact the spacecraft's weight, volume (array stowage), and system requirements on spacecraft attitude control systems (additional chemical fuel).

Three important figures of merit used in power system optimization are EOL area power density (W/m^2), specific weight (W/Kg), and cost ($/W). Representative values for the various SOA cell technologies are listed in Table 10.9.

The EOL power per unit area for a MJ cell is significantly better than a Si cell. However, the EOL specific weight for Si is almost a factor of two greater than a MJ cell. This results in a slightly smaller EOL cost per watt for a high-efficiency Si. This demonstrates the dramatic reduction in cost of MJ cells over the past few years.

If one considers the mass of the necessary array components (i.e. panel substrate, face sheet, adhesive, hinges, insulators, wiring, etc.) along with equivalent power per area for the different cell types, and also the cost involved in having the cells interconnected and covered (CIC) and laid on rigid panels, then the cost for developing an array using MJ cells is slightly less than that for HES cells. The EOL specific weight values at the CIC (with 100-μm ceria-doped microsheet cover glass) and the panel levels for these cells and the normalized cost per watt for the panels is shown in Table 10.10. A similar comparison with somewhat less expensive 100-μm high-efficiency Si cells (at the panel level) shows a slightly smaller cost advantage for the multijunction cells. The 100-μm Si

Table 10.9 EOL area power density (W/m^2), specific weight (W/Kg), and normalized (to HE Si) cost ($/W) for high-efficiency Si, dual-junction (2J), and triple-junction (3J) bare solar cells [52]

Solar cell technology	[W/m^2]	[W/Kg]	Normalized (to HE Si) cell cost [$/W]
GEO conditions (60°C) – 1-MeV, 5E14 e/cm²			
75 μm HE Si	169	676	1.00
2J III-V	271	319	1.38
3J III-V	306	360	1.22
LEO conditions (80°C) – 1-MeV, 1E15 e/cm²			
75 μm HE Si	143	574	1.00
2J III-V	245	288	1.29
3J III-V	275	323	1.15

Table 10.10 EOL specific weight (W/Kg) at the CIC and panel levels for three-mil high-efficiency Si, dual-junction (2J), and triple-junction (3J) cells [52]

Solar cell technology	CIC specific power [W/kg]	Panel specific power [W/kg]	Normalized (to HE Si) panel cost [$/W]
GEO conditions (60°C) – 1-MeV, 5E14 e/cm²			
75 μm H.E. Si	261	75	1.00
2J III-V	219	95	0.9
3J III-V	248	108	0.8
LEO conditions (80°C) – 1-MeV, 1E15 e/cm²			
75 μm H.E. Si	221	63	1.00
2J III-V	199	86	0.84
3J III-V	223	97	0.75

cells are less radiation-hard and have lower specific power (W/Kg) than 75-μm Si cells, but they cost about 35% less.

Currently conventional space Si cells are less expensive than MJ cells at the panel level. However, their EOL power is much lower than either the high-efficiency Si cells or the MJ cells. The increased mass and area that their usage entails would have to be considered against the cost savings and other mission considerations in any comparative study.

Engineers have worked on ways to improve space solar cells and arrays in terms of all the important figures of merit since the early days of our space program. Numerous mission studies have shown that even extremely high array costs can be worth the investment when they result in lower array mass. In general, mass saving in the power system can often be used by payload. If the revenue generated by this payload (i.e. more transmitters on a communications satellite) is greater than the cost of higher-efficiency solar cells, the choice is rather an easy one to make. However, often more instrument capabilities will require more support from the spacecraft (e.g. command and data handling, structure, attitude control, etc.) as well as more power. These additions can negate any apparent advantage to the overall spacecraft.

REFERENCES

1. Chapin D, Fuller C, Pearson G, *J. Appl. Phys.* **25**, 676–681 (1954).
2. Jenny D, Loeferski J, Rappaport P, *Phys. Rev.* **101**, 1208–1212 (1956).
3. Easton R, Votaw M, *Rev. Sci. Instrum.* **30**, 70–75 (1959).
4. Loeferski J, *J. Appl. Phys.* **27**, 777–785 (1956).
5. Jackson E, *Trans. of the Conf. on the Use of Solar Energy*, Vol. 5, 122–128 (Tucson, AZ, 1955).
6. *Bell Syst. Tech. J.* **42** (1963).
7. Solar Cell Array Design Handbook, *JPL* **SP43-38**, Vol. 1, 1.1–2 (1976).

8. Statler R, Curtin D, *Proc. International Conf. on the Sun in the Service of Mankind*, 361–367 (1973).
9. Reynolds D, Leies G, Antes L, Marburger R, *Phys. Rev.* **96**, 533 (1954).
10. Lebrun J, *Proc. 8th IEEE Photovoltaic Specialist Conf.*, 33–37 (1970).
11. North N, Baker D, *Proc. 9th IEEE Photovoltaic Specialist Conf.*, 263–270 (1972).
12. Bailey S, Raffaelle R, Emery K, *Proc. 17th Space Research and Technology Conf.* (2001).
13. Hague L *et al.*, *Proc. 31st Intersociety Energy Conversion Engineering Conf.*, 154–159 (1996).
14. Stella P *et al.*, *Proc. 34th Intersociety Energy Conversion Engineering Conf.* (1999).
15. Bailey S, Landis G, Raffaelle R, to be published in *The Proc. 6th European Space Power Conf.* (2002).
16. Bailey S *et al.*, *"Solar Cell and Array Technology for Future Space Science Missions"*, Internal NASA report to Code S (2002).
17. Bücher K, Kunzelmann S, *Proc. 2nd World Conference and Exhibition on Photovoltaic Solar Energy Conversion*, 2329–2333 (1998).
18. Green M *et al.*, *Prog. Photovolt.* **6**, 35–42 (1998).
19. Green M *et al.*, *Prog. Photovolt.* **9**, 287–293 (2001).
20. King R *et al.*, *Proc. 28th IEEE Photovoltaic Specialist Conf.*, 982–985 (2000).
21. Reynard D, Peterson D, *Proc. 9th IEEE Photovoltaic Specialist Conf.*, 303 (1972).
22. Crabb R, *Proc. 9th IEEE Photovoltaic Specialist Conf.*, 185–190 (1972).
23. Bailey S *et al.*, *Proc. 2nd World Conf. Photovoltaic Solar Energy Conversion*, 3650–3653 (1998).
24. Ferguson D, *Interactions between Spacecraft and their Environments*, AIAA Paper #93-0705, NASA TM 106115 (1993).
25. Landis G, Bailey S, *AIAA Space Sciences Meeting*, AIAA-2002-0718 (Reno, NV, 2002).
26. Flood D, *Proc. NHTC'00, 34th National Heat Transfer Conf.* (2000).
27. Anspaugh B, *GaAs Solar Cell Radiation Handbook*, 6–54, NASA JPL Publication 96-9 (1996).
28. Marvin D, Nocerino J, "*Degradation Predictions for Multijunction Solar Cells on Earth-Orbiting Spacecraft*", Aerospace Report No. TOR-2000(1210)-2, 9 (2000).
29. Walters R *et al.*, *Technical Digest of the International PVSEC-11*, 813–814 (1999).
30. Walters R, *Proc. 15th SPRAT*, 30–34 (1997).
31. Tada H, Carter J, Anspaugh B, Downing R, *Solar Cell Radiation Handbook*, 3–82, JPL Publication 82-69 (1982).
32. Fahrenbruch A, Bube R, *Fundamentals of Solar Cells*, Chap. 2, Academic Press, Boston (1983).
33. Landis G, *Proc. 13th SPRAT*, 385–399 (1994).
34. Scheiman D *et al.*, *Proc. 17th SPRAT Conference* (Cleveland, OH, Sept. 11–13, 2001).
35. Bailey S, Flood D, *Prog. Photovolt.* **6**, 1–14 (1998).
36. Keener D *et al.*, *Proc. 26th IEEE Photovoltaic Specialist Conf.*, 787–281 (1997).
37. Hoffman D *et al.*, *Proc. 35th IECEC*, AIAA-2000-2919 (2000).
38. Bailey S, Hepp A, Raffaelle R, *Proc. 36th Intersociety Energy Conversion Engineering Conference*, 235–238 (2001).
39. Guha S *et al.*, *Proc. 2nd World Conf. PV Solar Energy Conversion*, 3609–3612 (1998).
40. Deng X, Povolny H, Han S, Agarwal P, *Proc. 28th IEEE Photovoltaic Specialist Conf.*, 1050–1053 (2000).
41. Arya R *et al.*, *Proc. 1st World Conf. Photovoltaic Solar Energy Conversion*, 394–400 (1994).
42. Contrera M *et al.*, *Prog. Photovoltaics* **7**, 311–316 (1999).
43. Hanket G *et al.*, *Proc. 29th IEEE Photovoltaic Specialist Conf.*, 567–570 (1988).
44. Dhere N, Ghongadi S, Pandit M, Jahagirdar A, Scheiman D, *Prog. Photovoltaics* **10**, 407–416 (2002).
45. Romeo A, Blatzner D, Zogg H, Tiwari A, *Mat. Res. Soc. Symp. Proc.* Vol. 668, H3.3.1–3.6 (2001); results with 11% AM1.5 efficiency on polyimide have been submitted for publication.
46. Ferekides C *et al.*, *Thin Solid Films* 361–362, 520–526 (2000).
47. Marshall C *et al.*, *IECEC*, 1999-01-2550 (1999).

48. Messenger S *et al*., *Proc. 16th European Photovoltaic Energy Conference*, 974–977 (2000).
49. Tringe J, Merrill J, Reinhardt K, *Proc. 28th IEEE Photovoltaic Specialist Conf.*, 1242–1245 (2000).
50. Stella P, West J, *Proc. 21st IEEE Photovoltaic Specialist Conf.*, 1362–1366 (1990).
51. Gerlach L, Fournier-Sirce A, Fromberg A, Kroehnert S, *Proc. 21st IEEE Photovoltaic Specialist Conf.*, 1308–1312 (1990).
52. Scheiman D, Landis G, Weizer V, *AIP Conf. Proc.* **458**, 1–6 (1999).
53. Landis G, *Acta Astronautica* **38**, 1 (1996).
54. Larson W, Pranke L, Eds, *Human Spaceflight Mission Analysis and Design*, McGraw Hill, New York (1999).
55. Luque A, Marti A, *Phys. Rev. Lett.* **78**, 5014 (1997).
56. Leon R *et al*., *Appl. Phys. Lett.* **76**, 2071 (2000).
57. Hoffman D, Raffaelle R, Landis G, Hepp A, *Proc. 36th IECEC*, IECEC-2001-AT-21 (2001).
58. Raffaelle R *et al*., *Proc. 36th IECEC*, IECEC2001-AT-66 (2001).
59. Bailey S *et al*., *Proc. 17th Euro. Photovoltaic Solar Energy Conference*, 2137–2143 (2001).